Supplementary Material

Risks and mechanistic insights into arsenic-enhanced iodination of bisphenol F in *Brassica chinensis* L.

Kai Zheng [1], Tian Gao [1], Ke Li [1], Yina Guan [1], Shaoyang Hu [1], Yujiang Li [1], Chunguang Liu (✉)[1,2,3,4], Bing Yan[1]

1 School of Environmental Science and Engineering, Shandong Key Laboratory of Environmental Processes and Health, Shandong University, Qingdao 266237, China

2 Laboratory of Marine Ecological Environment in Universities of Shandong, Shandong University, Qingdao 266237, China

3 Qingdao Key Laboratory of Marine Pollutant Prevention, Shandong University, Qingdao 266237, China

4 Shandong Kenli Petrochemical Group Co., Ltd., Dongying 257000, China

Text. S1 The seeds of *Brassica chinensis L.* were disinfected with 10% H_2O_2 for 10 min and then soaked at 30℃ for 12 h. The seeds were germinated in the dark at 26℃ for two days following soaking. After germination, the *Brassica chinensis L.* seeds were moved to a 100% Hoagland nutrient solution for hydroponic cultivation, exposed to an 18/6 h light/dark cycle with a light intensity of 15000 lx (full spectrum) and temperatures of 26℃/24℃ (Dong et al., 2023). Every two days, the nutrient solution was replaced. After two weeks, the irrigation was altered to a 25% nutrient solution

Text. S2 After 45 days, *Brassica chinensis L.* with consistent growth size was selected for experimentation. The experimental group received a complex Hoagland nutrient solution with I^-, BPF, and different levels of As(V). KI was concentrated at 40 μmol/L, BPF at 3 mg/L, and $Na_2HAsO_4 \cdot 7H_2O$ at 0, 25, 50, and 100 μmol/L. Three separate groups were set up with the inclusion of a peroxidase inhibitor (SHAM, 150 μmol/L) (Mei et al., 2009; Graças et al., 2016), an NADPH oxidase inhibitor (DPI, 15 μmol/L) (Li et al., 2017; Tian et al., 2017; Xiao et al., 2021), and a hydrogen peroxide scavenger (4-hydroxy-Tempo, 40 μmol/L) (Wang et al., 2022). The inhibitor concentration was chosen within a range identified in the existing literature and further validated through preliminary experiments. Following a 5-day exposure period, samples were collected for analysis

✉ Corresponding author
E-mail: chunguangliu2013@sdu.edu.cn

Text. S3 The supernatant was collected and filtered through a 0.22 μm membrane to remove most peroxidases and other macromolecular proteins. The filtrate was passed through an activated solid-phase extraction (SPE) column to remove pigments, organic substances, and macromolecular proteins. The SPE column was pre-activated by washing three times with 5 mL of methanol and three times with 5 mL of 0.1% formic acid using a solid-phase extraction device (HSE-12B) (detailed procedures shown in Fig. S1). The solution was then passed through a second activated SPE column, which was pre-activated by washing three times with 5 mL of methanol and three times with 5 mL of ultrapure water (using the same method as the first column). This step removed small organic molecules, leaving only inorganic ions in the liquid

Text. S4 The frozen HepG2 cells were resuscitated. HepG2 cells were cultured in modified Eagle medium (DMEM) with 10% fetal bovine serum (FBS), 2 mmol/L L-glutamine, 50 mmol/L sodium pyruvate, 1 g/L glucose, 100 UI/mL penicillin, 0.1 mg/mL streptomycin, and maintained in a humidified atmosphere 5% CO_2 and 95% air at 37℃. Experiments were performed by passaging cultured HepG2 cells three times

Table S1 The molecular mass and catalog numbers of the chemicals used in this research.

Chemicals	Molecular mass	CAS	Purity
Bisphenol F	200.2370	620-92-8	⩾98%
Sodium hydrogen arsenate heptahydrate	312.0140	10048-95-0	⩾98%
Dimethyl-p-phenylenediamine	136.1940	99-98-9	⩾98%
Diphenyleneiodonium chloride	316.5700	4673-26-1	⩾98%
Salicylhydroxamic acid	153.1400	89-73-6	⩾98%
4-Hydroxy Tempo	172.2400	2226-96-2	⩾98%
Acetonitrile	41.0500	75-05-8	⩾99%
Hydrogen peroxide	34.0147	7722-84-1	⩾30%
Sodium Phosphate, Dibasic	141.9600	7558-79-4	⩾99%
sodium dihydrogen phosphate anhydrous	119.9770	7558-80-7	⩾99%
Potassium iodide	166.0000	7681-11-0	⩾99%
Methyl alcohol	32.0400	67-56-1	⩾99%

Table S2 q-PCR verified the primer sequences of genes common to the selected roots and leaves and the internal standard genes.

Primer	Primer sequence (5′to3′)
Bra008510-F	TCTTCTTCTCCATCTCCTCCTC
Bra008510-R	CCACCAGATGGTTCCGATAAA
Bra017830-F	GACTTGGAGTAGGGTTGTGATG
Bra017830-R	CCATCTCCGGCCAATGATAAA
Bra024875-F	CTTCTACGAGACTTGCCCTTAC
Bra024875-R	GATGACGTGGACTCTCTTCTTC
Bra038612-F	CGGATCATCGAAGAGAGTCATC
Bra038612-R	CCATACGAACCTGGGAGAATAG
CyP-F	AGGAGGAGATTTCACCGC
CyP-R	TCTCTAACGACATCCATCCC

Table S3 Gaussian 09W calculates $2FED^2_{HOMO}$ per carbon before iodine electrophilic substitution.

TP1-1	TP2-1	TP3-1	TP4	TP4-1 TP5-1	TP6-1	TP7-1
1C	1C	1C	1C	1C	1C 0.109400	1C
0.022844	0.030885	0.237327	0.002860	0.119868		0.072379
2C	2C	2C	2C	2C	2C 0.048701	2C
0.072846	0.152603	0.017934	0.009573	0.022765		0.018790
3C	3C	3C	3C	3C	3C 0.049076	3C
0.081990	0.153311	0.146519	0.010431	0.053720		0.011784
4C	4C	4C	4C	4C	4C 0.097197	4C
0.032993	0.001932	0.140240	0.005546	0.081960		0.033891
5C	5C	5C	5C	5C	5C 0.049738	5C
0.047022	0.158617	0.084254	0.004514	0.052687		0.030405
6C	6C	6C	6C	6C	6C 0.062131	6C
0.145564	0.111347	0.040329	0.017332	0.032963		0.015635
7C	7C	7C	7C	7C	7C 0.109400	7C
0.010875	0.022369	0.001601	0.003094	0.009974		0.006717
8C	8C		8C	8C	8C 0.048706	8C
0.146688	0.004646		0.013833	0.008959		0.124959
9C	9C		9C	9C	9C 0.049065	9C
0.023000	0.021277		0.121133	0.120817		0.022947
10C	10C		10C	10C	10C	10C
0.073161	0.021213		0.073016	0.021383	0.097196	0.069816
11C	11C		11C	11C	11C	11C
0.082546	0.002565		0.279431	0.056502	0.049750	0.087545
12C	12C		12C	12C	12C	12C
0.033372	0.056523		0.037531	0.082387	0.062129	0.052482
13C	13C		13C	13C		13C
0.047141	0.010098		0.159506	0.050942		0.032746
			^{14}C	^{14}C		^{14}C
			0.165689	0.034351		0.066990
						15C
						0.036305
						16C
						0.019402
						17C
						0.053247
						18C
						0.046869
						19C
						0.049975

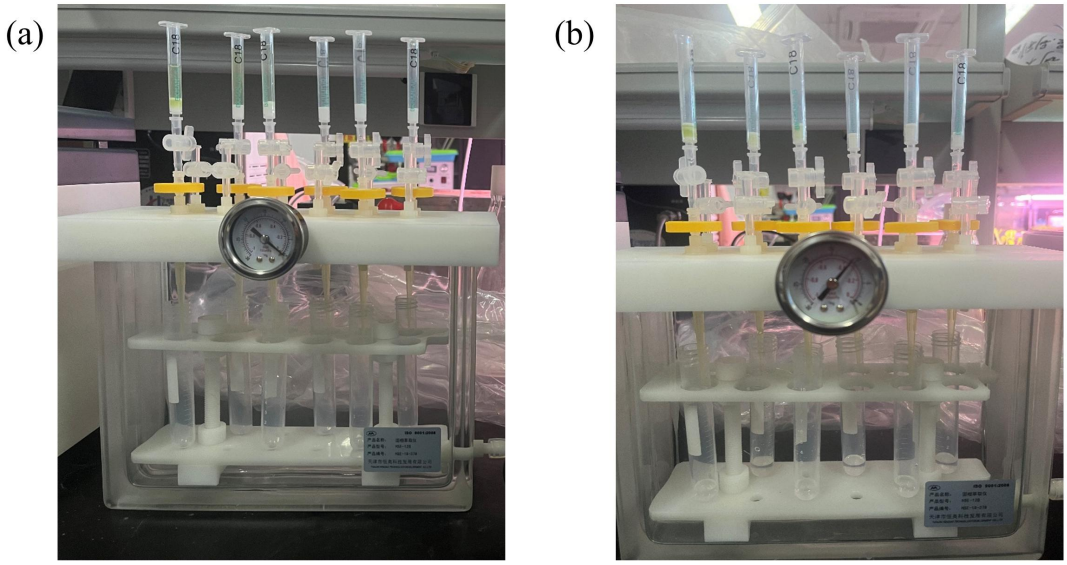

Fig. S1 Diagram of the operation of the C18 solid-phase extraction column for RIS pretreatment: (a) Before liquid pretreatment; (b) After liquid pretreatment.

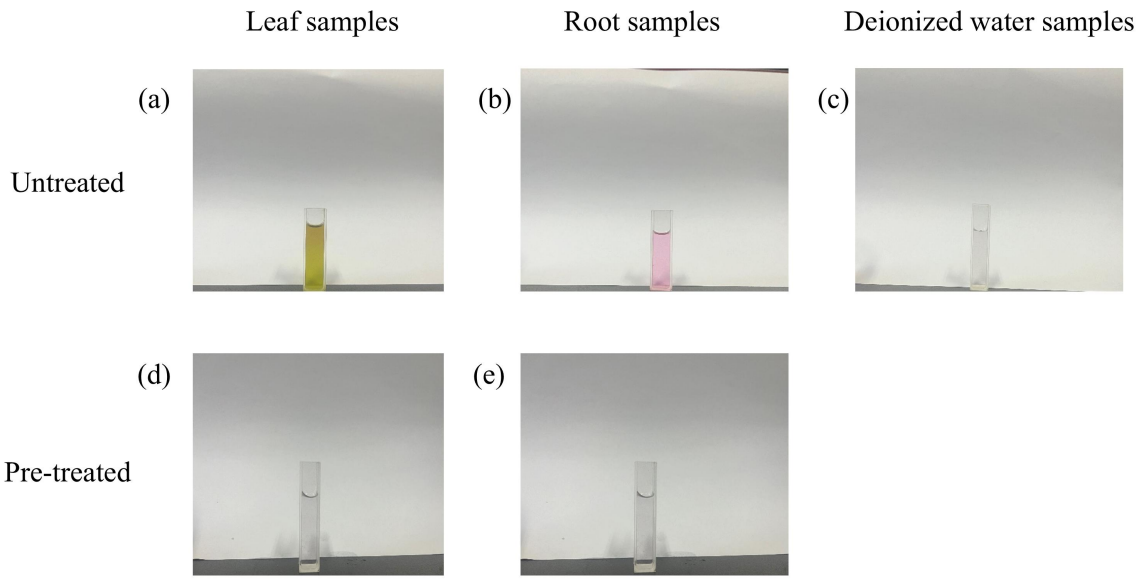

Fig. S2 Color change of roots and leaves of *Brassica chinensis L.* in the absence of contaminant exposure with and without pretreatment and DPD reaction compared to deionized water: (a) Schematic diagram of leaf samples without pretreatment; (b) Schematic diagram of root samples without pretreatment; (c) Schematic diagram of deionized water samples without pretreatment; (d) Schematic diagram of leaf samples with pretreatment; (e) Schematic diagram of root samples with pretreatment.

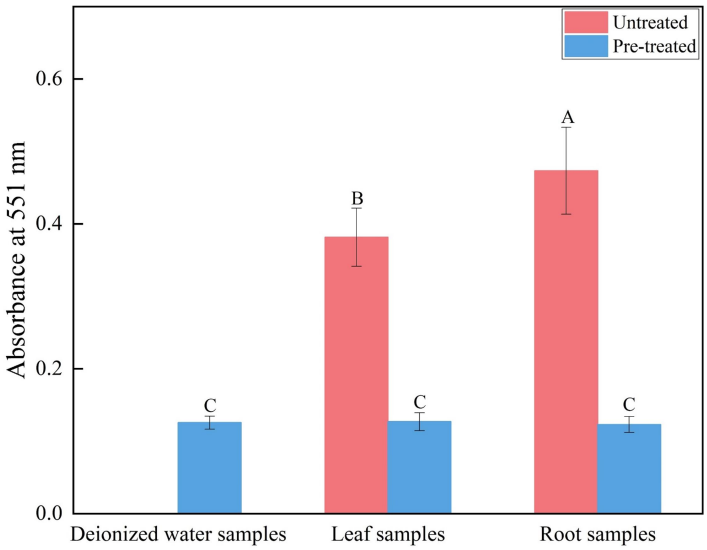

Fig. S3 Changes in absorbance of roots and leaves of *Brassica chinensis L.* in the absence of contaminant exposure with and without DPD compared to deionized water. The letter labeling method was used in the figure to present the results of difference analysis. Groups labeled with different letters indicate statistically significant differences ($p < 0.05$), while groups sharing the same letter indicate no significant differences.

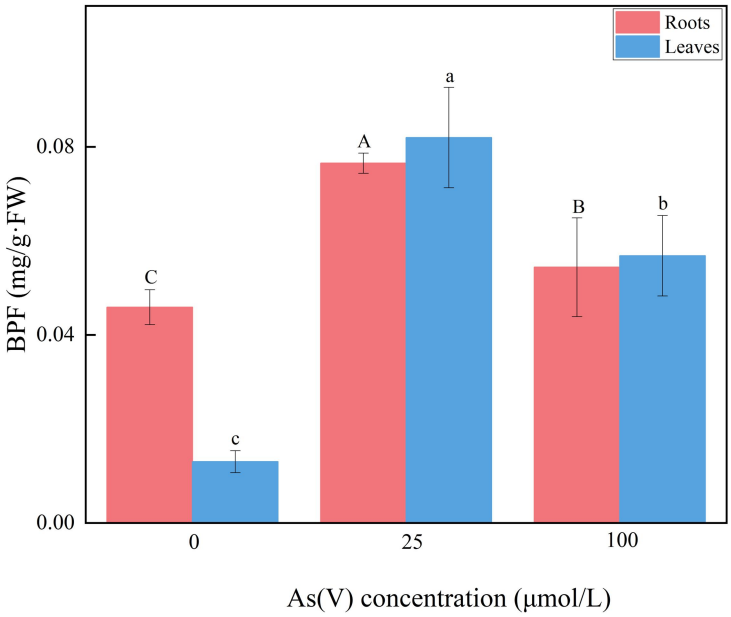

Fig. S4 BPF content in roots and leaves of *Brassica chinensis L.* under different As(V) treatments. C_{BPF} = 3 mg/L, C_{I^-} = 40 μmol/L. The letter labeling method was used in the figure to present the results of difference analysis. Groups labeled with different letters indicate statistically significant differences ($p < 0.05$), while groups sharing the same letter indicate no significant differences. In the figure, uppercase letters represent root groups, and lowercase letters represent leaf groups.

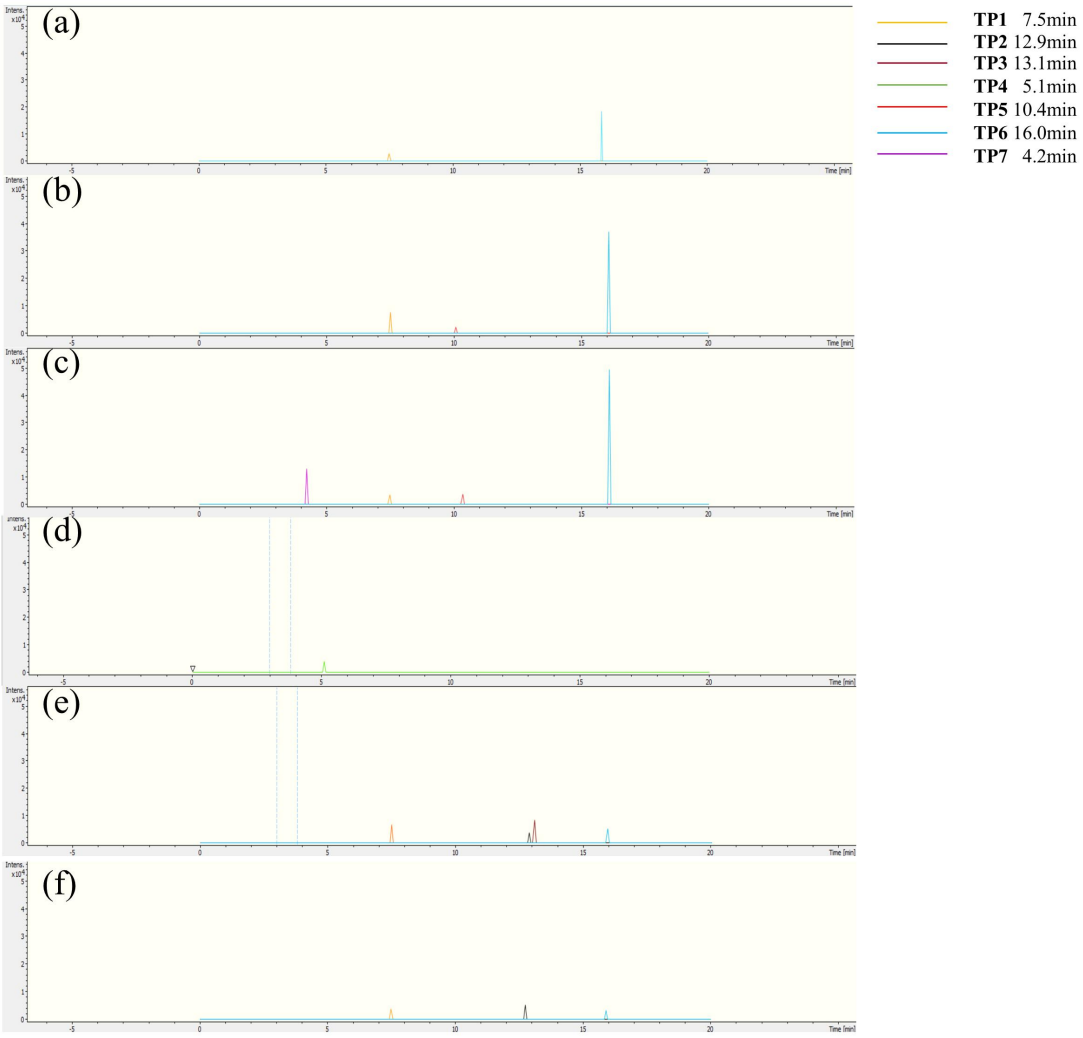

Fig. S5 Extracted Ion Chromatograms (EIC) summarizing the profiles of iodinated products in the roots (a–c) and leaves (d–f) of *Brassica chinensis L.* under different As(V) treatments (0, 25, and 100 μmol/L corresponding to a–c for roots and d–f for leaves, respectively).

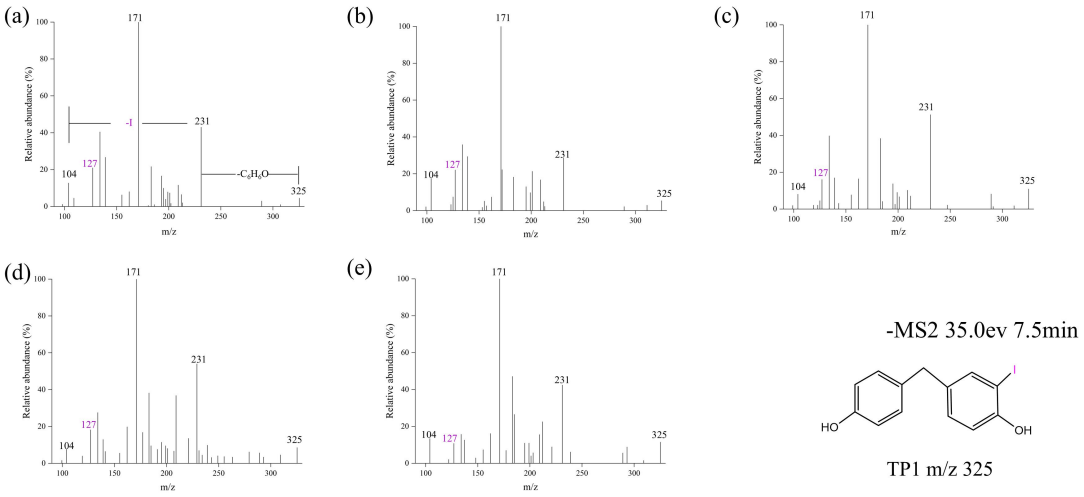

Fig. S6 Secondary mass spectrum of TP1 at As(V) concentration of (a) 0 μmol/L; (b) 25 μmol/L; (c) 100 μmol/L in roots and (d) 25 μmol/L; (e) 100 μmol/L in leaves.

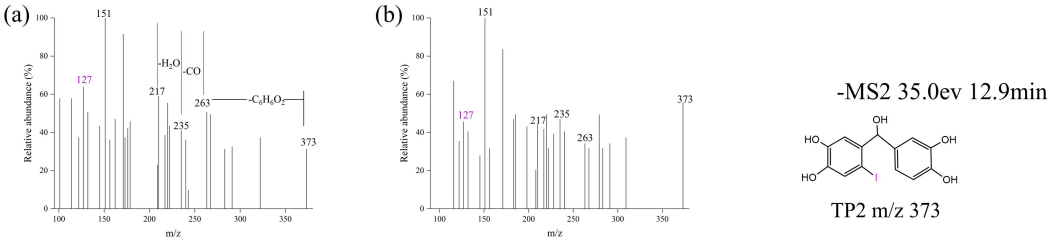

Fig. S7 Secondary mass spectra of TP2 in leaves at As(V) concentrations of (a) 25 μmol/L and (b) 100 μmol/L.

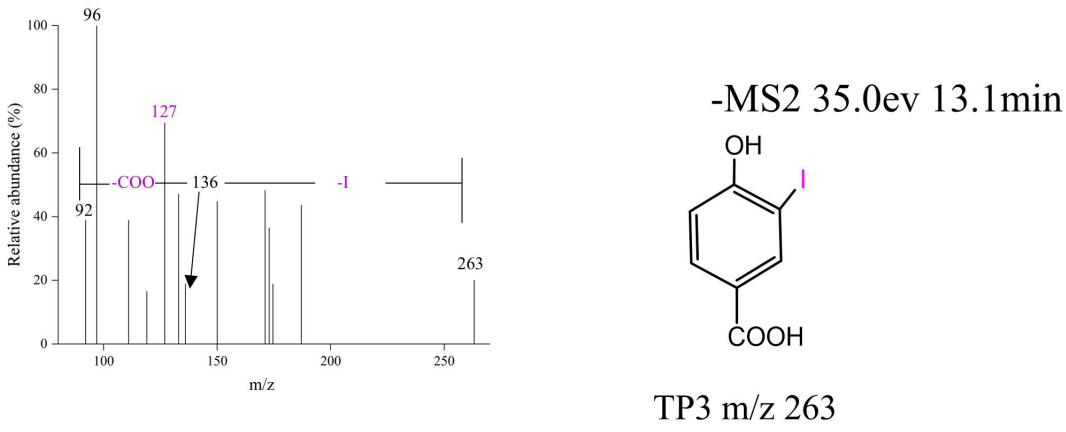

Fig. S8 Secondary mass spectrum of TP3 in leaves at 25 μmol/L As(V).

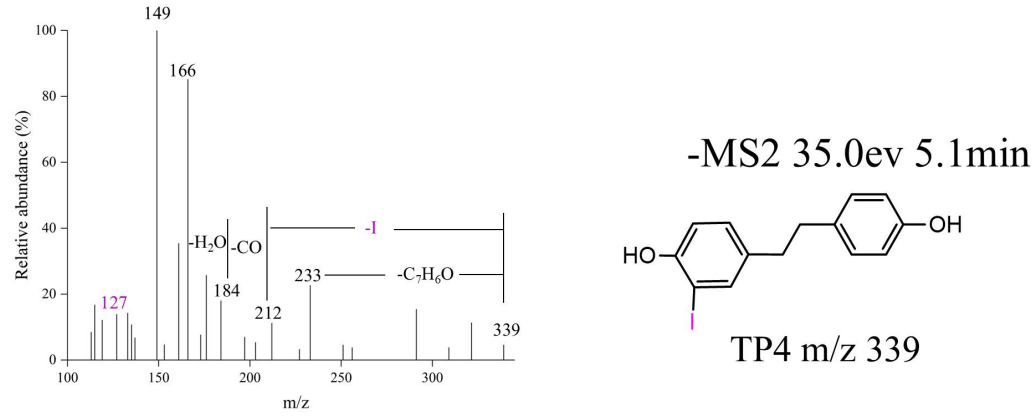

Fig. S9 Secondary mass spectrum of TP4 in leaves at 0 μmol/L As(V).

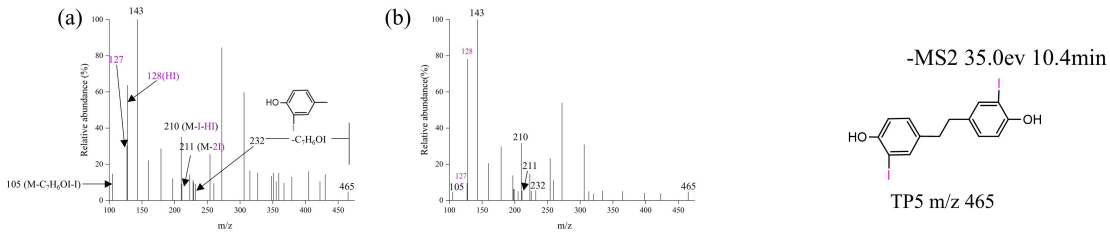

Fig. S10 Secondary mass spectra of TP5 in roots at As(V) concentrations of (a) 25 μmol/L and (b) 100 μmol/L.

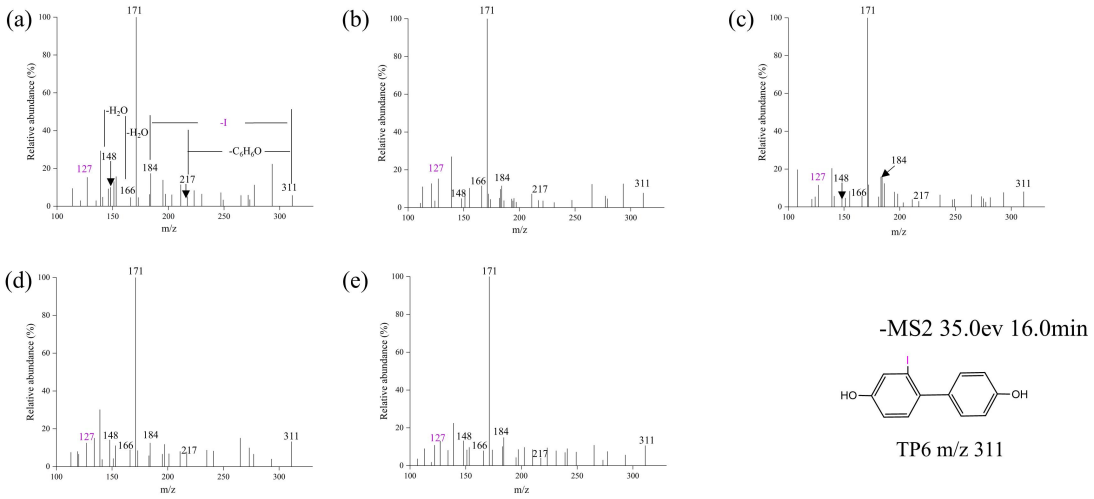

Fig. S11 Secondary mass spectrum of TP6 at As(V) concentration of (a) 0 μmol/L; (b) 25 μmol/L; (c) 100 μmol/L in roots and (d) 25 μmol/L; (e) 100 μmol/L in leaves.

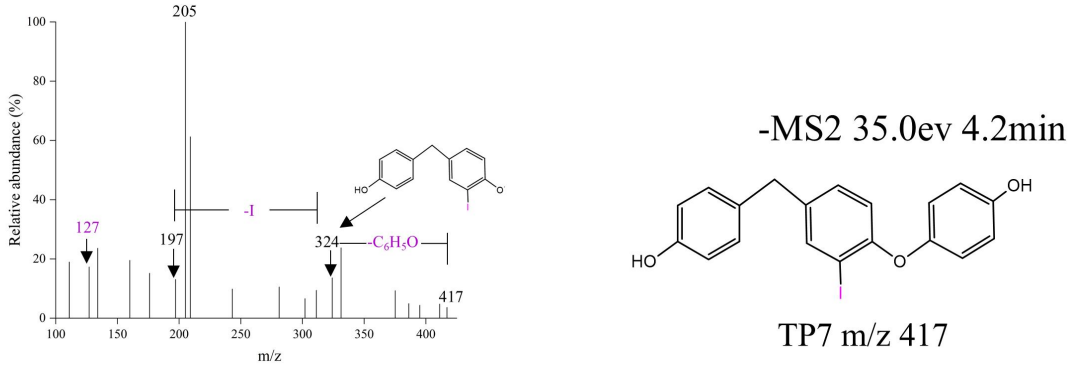

Fig. S12 Secondary mass spectrum of TP7 in roots at 100 μmol/L As(V).

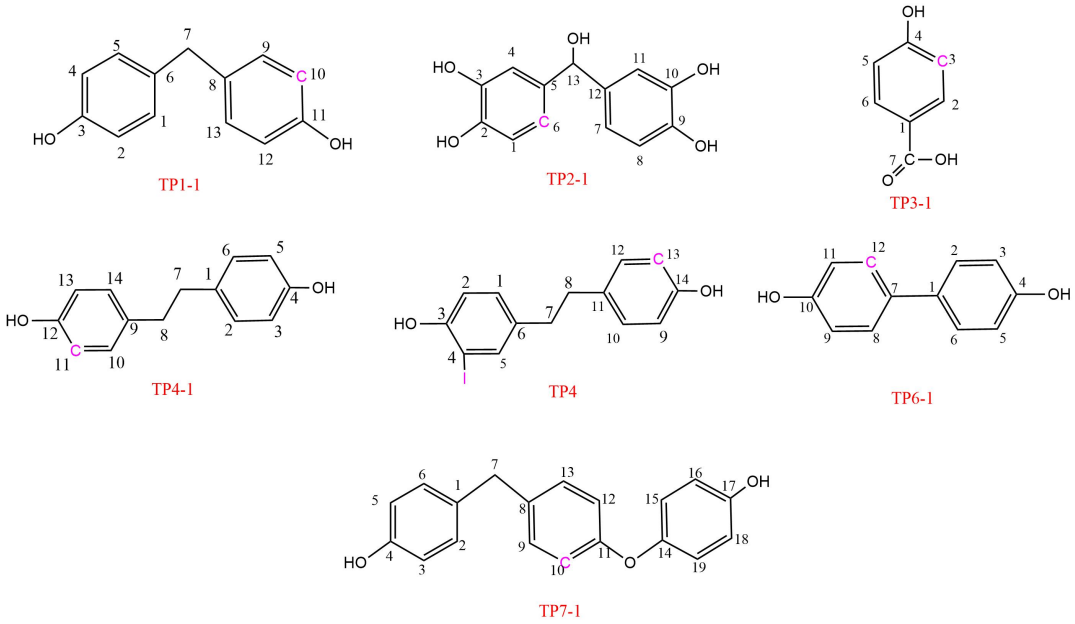

Fig. S13 Calculate C atoms with the highest $2FED^2_{HOMO}$ values in various iodide products using Gaussin 09W, as shown in purple C.

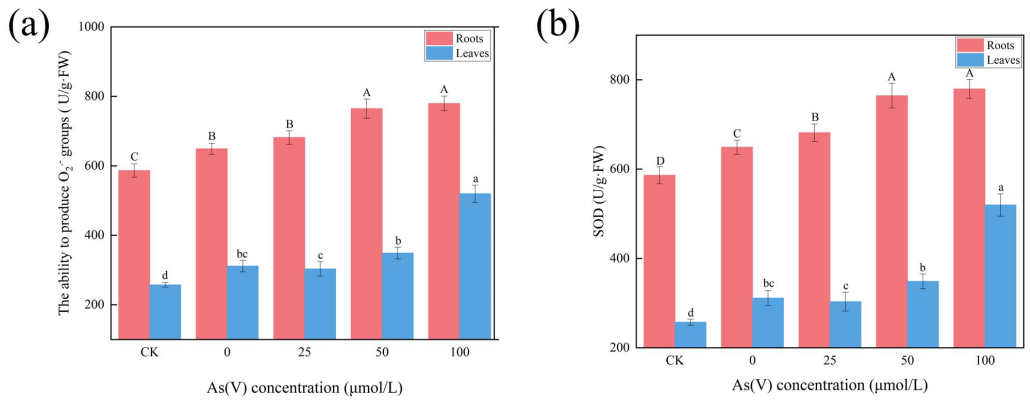

Fig. S14 Changes in superoxide anion production (a) and SOD enzyme activity (b) in roots and leaves of *Brassica chinensis L.* under different As(V) treatments. C_{BPF} = 3 mg/L, C_{I^-} = 40 μmol/L. The letter labeling method was used in the figure to present the results of difference analysis. Groups labeled with different letters indicate statistically significant differences ($p < 0.05$), while groups sharing the same letter indicate no significant differences. In the figure, uppercase letters represent root groups, and lowercase letters represent leaf groups.

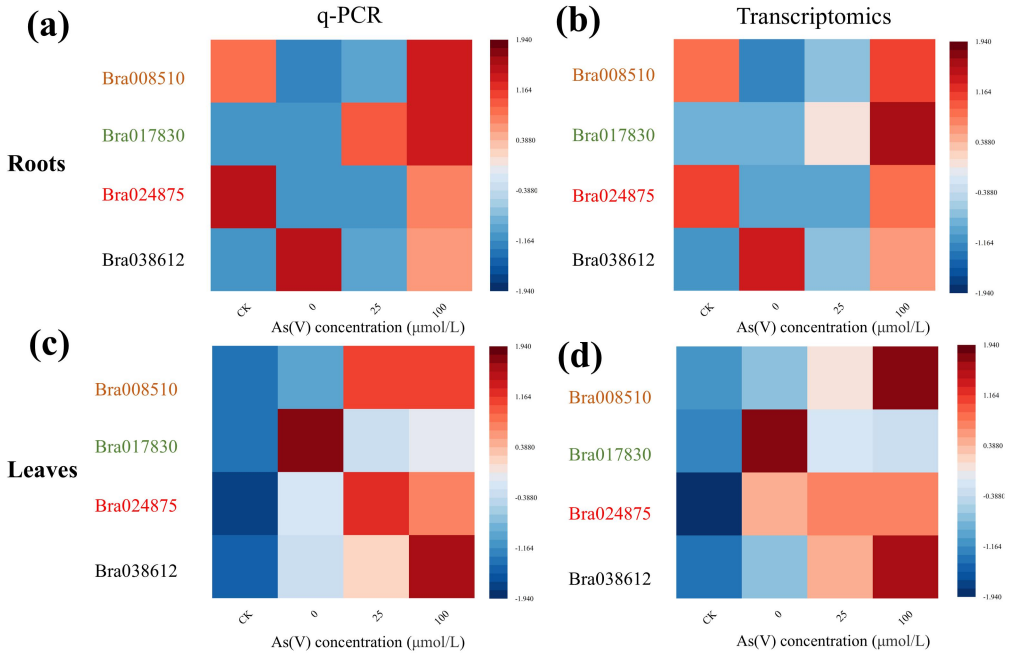

Fig. S15 Under different concentrations of As(V) treatment, genes shared in roots and leaves were selected for q-PCR validation and comparison of transcriptomic results: (a) Expression results of genes in roots by q-PCR. (b) The expression results of transcriptomics of genes in roots. (c) The expression results of q-PCR genes in leaves. (d) Transcriptomic expression results of genes in leaves.

References

Dong M, Sun N, Liu C (2023). Bromide ion enhancing the phytodegradation of emerging phenolic pollutants and its mechanisms mediating wheat resistance to phenolic pollutants stress. Journal of Cleaner Production, 411: 137295

Graças J P, Ruiz-Romero R, Figueiredo L D, Mattiello L, Peres L E P, Vitorello V A (2016). Root growth restraint can be an acclimatory response to low pH and is associated with reduced cell mortality: a possible role of class III peroxidases and NADPH oxidases. Plant Biology, 18(4): 658–668

Li W Y, Chen B X, Chen Z J, Gao Y T, Chen Z, Liu J (2017). Reactive oxygen species generated by NADPH oxidases promote radicle protrusion and root elongation during rice seed germination. International Journal of Molecular Sciences, 18(1): 110

Mei W, Qin Y, Song W, Li J, Zhu Y (2009). Cotton GhPOX1 encoding plant class III peroxidase may be responsible for the high level of reactive oxygen species production that is related to cotton fiber elongation. Journal of Genetics and Genomics, 36(3): 141–150

Tian J, Cheng Y, Kong X, Liu M, Jiang F, Wu Z (2017). Induction of reactive oxygen species and the potential role of NADPH oxidase in hyperhydricity of garlic plantlets in vitro. Protoplasma, 254(1): 379–388

Wang K, Yu H, Zhang X, Ye D, Huang H, Wang Y, Zheng Z, Li T (2022). Hydrogen peroxide contributes to cadmium binding on root cell wall pectin of cadmium-safe rice line (*Oryza sativa* L.). Ecotoxicology and Environmental Safety, 237: 113526

Xiao Y, Zhang L, Zhang H, Feng H, Li Z, Chen H (2021). Interaction between endogenous H_2O_2 and $OsVPE_3$ in the GA-induced PCD of rice aleurone layers. Plant Cell Reports, 40(4): 691–705